



This article appeared in a journal published by Elsevier. The attached copy is furnished to the author for internal non-commercial research and education use, including for instruction at the authors institution and sharing with colleagues.

Other uses, including reproduction and distribution, or selling or licensing copies, or posting to personal, institutional or third party websites are prohibited.

In most cases authors are permitted to post their version of the article (e.g. in Word or Tex form) to their personal website or institutional repository. Authors requiring further information regarding Elsevier's archiving and manuscript policies are encouraged to visit:

<http://www.elsevier.com/copyright>



Contents lists available at SciVerse ScienceDirect

Int. Journal of Refractory Metals and Hard Materials

journal homepage: www.elsevier.com/locate/IJRMHM

Short communication

X-ray diffraction evidence of a phase transformation in zirconia by the presence of graphite and carbon nanotubes in zirconia toughened alumina composites

M.H. Bocanegra-Bernal^{a,*}, A. Reyes-Rojas^a, A. Aguilar-Elguézabal^a, E. Torres-Moye^a, J. Echeberria^b^a Centro de Investigación en Materiales Avanzados, CIMAV S.C., Laboratorio Nacional de Nanotecnología, Miguel de Cervantes # 120 Complejo Industrial Chihuahua 31109, México^b CEIT and TECNUN (University of Navarra), 20018 San Sebastian, Spain

ARTICLE INFO

Article history:

Received 25 May 2012

Accepted 17 July 2012

Keywords:

Zirconia toughened alumina

Carbon nanotubes

Graphite

Monoclinic phase transformation

Rietveld

ABSTRACT

We have demonstrated by X-ray diffraction a transformation from the *t*-ZrO₂ phase into the *m*-ZrO₂ phase by the presence of multiwall carbon nanotubes (MWCNTs) and graphite powder (GP) in zirconia toughened alumina composites sintered in air. The phase transformation does not occur in sintering under an argon atmosphere. The quantitative phase analysis was carried out by fitting the X-ray diffraction profile with the Rietveld method making use of the FullProf software. The obtained amounts of *m*-ZrO₂ phase by the presence of GP and MWCNTs were 5% and 2.2%, respectively, at a sintering temperature of 1520 °C for 1 h.

© 2012 Elsevier Ltd. All rights reserved.

1. Introduction

Among advanced ceramics, zirconia (ZrO₂) has found applications in the industry and technology because of their unusual combination of strength, fracture toughness and chemical resistance. ZrO₂ has three polymorphic crystalline structures, namely, monoclinic *m* (below 1170 °C), tetragonal *t* (between 1170 °C and 2370 °C) and cubic *c* (above 2370 °C). This high temperature *c*-phase can be stabilized to room temperature by incorporating some oxide systems as dopants such as CaO, MgO, Y₂O₃, CeO₂ [1–4].

On the other hand, the results obtained for ZrO₂-SiN₃ and ZrO₂-SiC have been relatively poor compared to oxide systems. A stabilization of zirconia by nitrogen or by solid nitrides has been observed after ZrO₂ is sintered in nitrogen atmosphere [5]. The influence of carbon on the phase structure and stability of ZrO₂ has been studied by Wang et al. [6] who described that *t*-ZrO₂ would be obtained by carburizing the pure *m*-ZrO₂ powder at 1500 °C. However, the influence of carbon on this phase stability is still unclear. Herein, after a detailed and careful experimentation we provide experimental evidence of a phase transformation from the *t*-ZrO₂ into the *m*-ZrO₂ phase by GP and CNTs presence, this unusual behavior demands the contribution of the scientific community to elucidate a proper explanation of this phase transformation.

2. Experimental procedure

Since the experimental procedure has been described in detail elsewhere [7], it will be explained briefly here. The compositions tested

here were indicated as C1 (Al₂O₃ + 0.025 wt.% MgO + 13 wt.% ZrO₂ (Tosoh 3Y) + 2 wt.% *m*-ZrO₂), C2 (Al₂O₃ + 0.025 wt.% MgO + 13 wt.% ZrO₂ (Tosoh 3Y) + 2 wt.% *m*-ZrO₂ + 0.01 wt.% MWCNTs) and C3 (ZrO₂ (Tosoh 3Y) + 0.025 wt.% MgO + 13 wt.% Al₂O₃ + 2 wt.% *m*-ZrO₂ + 0.01 wt.% MWCNTs). The as-received powders and MWCNTs were carefully dispersed in ethanol with ultrasonic agitation for 2 h followed by magnetic stirring until most of ethanol evaporated and then the mixture was dried. The agglomerated mixture was ground intense and carefully in an agate mortar. Each mixture was uniaxially pressed at 50 MPa in a disk (steel die) with 16 mm diameter at a constant strain rate. Green samples with additions of MWCNTs were confined into an alumina sagger with high purity graphite packing powder (graphite powder, crystalline, – 300 mesh, 99%, Alfa Aesar), where the alumina powder fill the space between the two high alumina crucibles. A third crucible covers the one containing the graphite bed powder with the sample. Samples without additions of MWCNTs were directly set into Al₂O₃ crucible with ZrO₂ + Al₂O₃ bed powder. The sintering temperature range varied from 1400 °C to 1600 °C for various soaking times from 1 h to 10 h in air atmosphere. The samples were ground and polished by SiC paper and then polished by diamond pastes of both 0.5 and 0.25 μm. Details on X-ray diffraction (XRD) conditions are given in the Supplementary material.

3. Results and discussion

Fig. 1 presents the XRD patterns of the composition C2 sintered in air using GP as bed powder (pattern # 1) and argon atmosphere (pattern # 2). Two significant peaks corresponding to the *m*-ZrO₂ can be observed in the sample sintered with graphite bed powder (pattern # 1) in comparison to the pattern of the sample sintered in

* Corresponding author. Tel.: +52 614 4394801; fax: +52 614439 4852.

E-mail address: miguel.bocanegra@cimav.edu.mx (M.H. Bocanegra-Bernal).

argon (pattern # 2). It is clearly observed that some of the t -ZrO₂ was transformed into m -ZrO₂ after sintering.

To evaluate separately the contribution of GP and CNTs to the transformation of the t -ZrO₂ to the m -ZrO₂ phase, the unpolished (“as sintered”) sample C1 was sintered at the same temperature (1520 °C) for 1 h in air (Fig. 2a) as well as using GP as bed powder at different times (Fig. 2b). Following the same procedure, the “as received” sample C2 was also sintered at 1520 °C using GP as bed powder (Fig. 2c) at the same times that the C1 (Fig. 2b). When C1 was sintered in air (Fig. 2a), only the t -ZrO₂ phase is present while the m -ZrO₂ phase has appeared when C1 has been sintered in air but using GP as bed powder. Newly, a transformation of the t -ZrO₂ has occurred by the presence of GP. Nonetheless, the m -ZrO₂ phase present in the patterns of the Fig. 2c corresponding to the C2 sample (with CNTs content) must be the contribution of both GP and CNTs. The crystallographic data obtained with Rietveld fitting profile XRD patterns of sintered samples in air and using GP as bed powder is shown in Fig. 3. The lower curve in the graph (Fig. 3a) corresponds to the difference between the observed and calculated intensity, plotted on the same scale. The m -ZrO₂ and t -ZrO₂ peaks are shown in more detail in Fig. 3b. The percentages corresponding to α -Al₂O₃, t -ZrO₂ and m -ZrO₂ are shown in Table 1. From this Table 1 can be seen that the GP and the CNTs contributed to the transformation of the t -ZrO₂ phase to the m -ZrO₂ phase in amounts of 5.0% and 2.2%, respectively.

We have also observed that to obtain satisfactory stability in the t -ZrO₂ phase, the presence of certain concentrations of stabilizing oxide is required. However, there are also limits to the grain size and the “mechanical” constraints of grain boundaries to stabilize the t -ZrO₂ phase against displacive phase transformation. This is entirely consistent with experience across a range of systems exhibiting displacive or martensitic transformations, where the applications of suitable applied stress or mechanical constraint can stabilize the parent phase against the transformation [8]. In our samples, the bulk matrix constraints are already relaxed to a significant degree in the vicinity of the free surface. If the CNTs are such as to further reduce or relax the “mechanical” constraint on the t -ZrO₂ phase, then it could well explain the apparent transformation of the t -ZrO₂ phase and formation of the m -ZrO₂ phase. However, we also observed that polishing the sintered surfaces, the m -ZrO₂ phase can be removed from the surface. This seems to suggest that there is some surface reaction during sintering that contributes to the transformation of the surface t -ZrO₂ phase in the “as sintered” samples. If it were purely due to the mechanical relaxation, then we would have expected that as soon as we expose fresh surface, the surface t -ZrO₂ would be

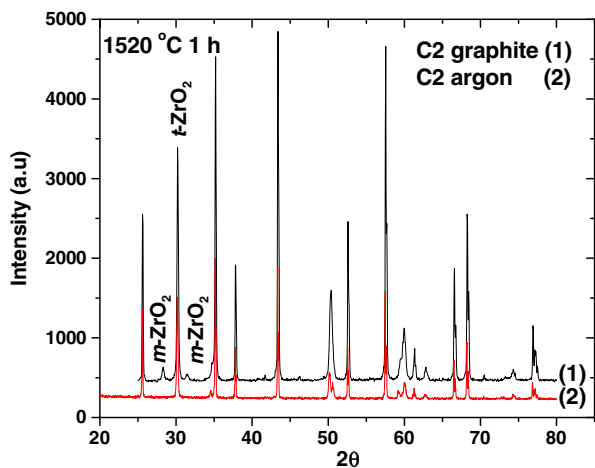


Fig. 1. XRD patterns of sintered sample C2 sintered at 1520 °C for 1 h.

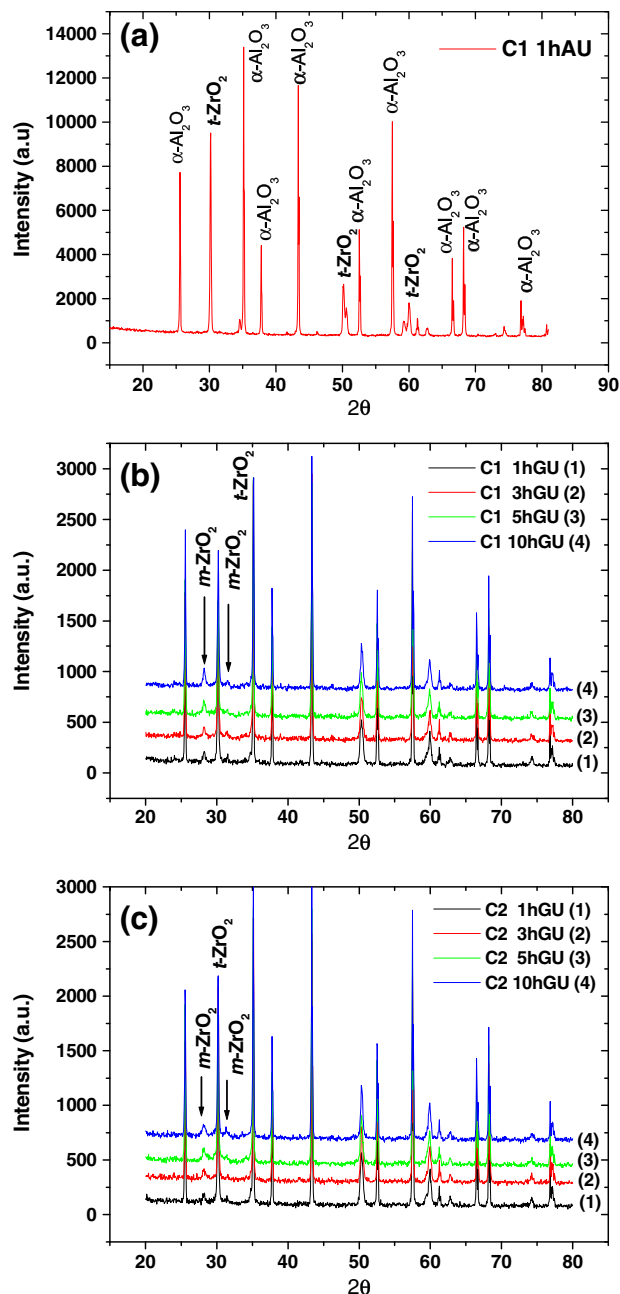


Fig. 2. XRD patterns of samples sintered at 1520 °C. (a) Sample C1 1 h, (b) Sample C1 and (c) sample C2 sintered at four different sintering times. A = air; h = hours; G = graphite bed powder; U = unpolished surface.

locally transformed. The Supplementary Figs. S1a and S1b show the XRD patterns corresponding to the polished surfaces of the “as sintered” C1 and C2 samples, respectively. It is clear that the m -ZrO₂ phase has practically disappeared.

The polished samples C1 and C2 were re-sintered under same sintering conditions. As can be seen in the XRD patterns of the Fig. 4a and b, the m -ZrO₂ phase was formed indicating as mentioned earlier that the exposition of fresh surface destabilize the surface t -ZrO₂ being more notorious this phenomenon with the sample C2 which contain CNTs (Fig. 4b). To corroborate if the phase transformation could occur in the surface only, a sample C2 sintered at 1520 °C for 1 h using GP as bed powder was cut in traverse section and analyzed by XRD. The pattern is shown in the Fig. 5a where a small peak assignable to the m -ZrO₂ phase is present suggesting probably

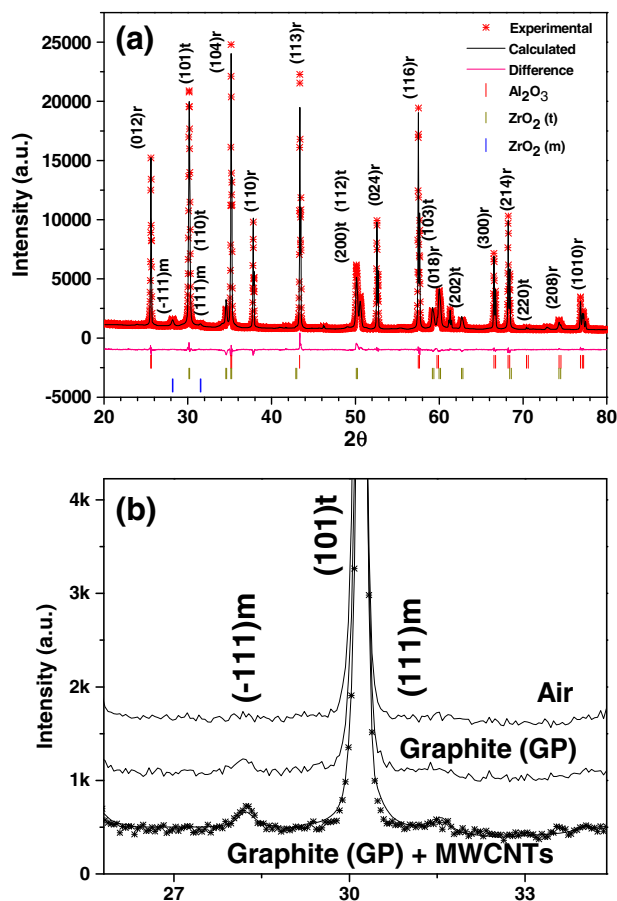


Fig. 3. (a): Rietveld plot of refinement results for samples C1 and C2 sintered at 1520 °C for 1 h. (b): Enlarged 2θ range between 27 and 33 where the (−111)*m*, (101)*t* and (111)*m* planes are identifiable. (Air=Sample C1 sintered in air without graphite bed powder; Graphite (GP)=Sample C1 sintered in graphite bed powder; Graphite (GP)+MWCNTs=Sample C2 sintered in graphite bed powder).

that the phase transformation in the bulk will occur due to the carbon nanotubes presence. The enlarged square in Fig. 5a is shown in Fig. 5b.

It is noteworthy that our results presented here are in disagreement with the pointed out by Luo et al. [6,9] who reported that the addition of CNTs would be propitious to the transition from *m*-ZrO₂ to *c*-ZrO₂ and to the stabilization of cubic ZrO₂ and Wang and Liang [10] who revealed an increasing of the *t*-ZrO₂ content in pure *m*-ZrO₂, 2Y-TZP and 3Y-TZP. According to the diffraction patterns showed here, it is evident that there is a transformation of the tetragonal zirconia phase during sintering in the presence of GP and CNTs. Therefore, in the light of this experimental evidence and taking into account that the

Table 1
m-ZrO₂ phase content in the samples C1 and C2 sintered at 1520 °C for 1 h. (estimated standard deviation values given in parentheses refer to the least significant digit).

Phase	(a) Air	(b) Graphite (GP)	(c) Graphite (GP) + MWCNTs
α-Al ₂ O ₃	76.9(3)	76.7(4)	76.3(1)
<i>t</i> -ZrO ₂	23.1(4)	18.3(2)	16.5(2)
<i>m</i> -ZrO ₂		5.0(1)	7.2(2)

(a) Air: Sample C1 sintered in air at 1520 °C without graphite bed powder.
(b) Graphite (GP): Sample C1 sintered at 1520 °C using graphite bed powder.
(c) Graphite (GP)+MWCNTs: Sample C2 sintered at 1520 °C using graphite bed powder.

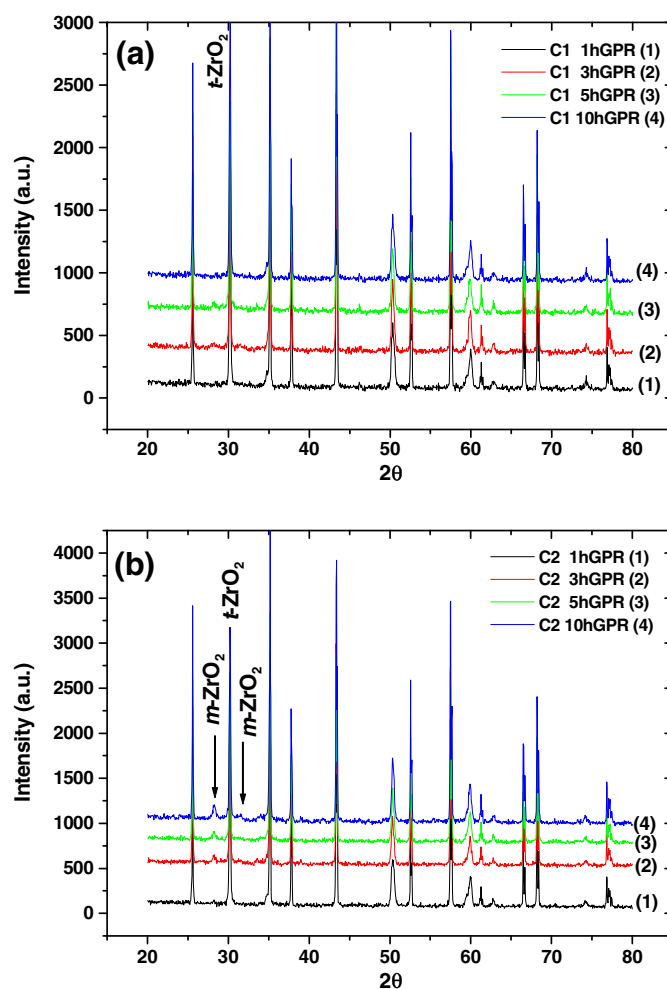


Fig. 4. XRD diffractograms of samples sintered and resintered at 1520 °C at four different times after polishing surfaces. (a) Sample C1 and (b) Sample C2. Note in (b) the appearance of the *m*-ZrO₂ phase after resintering treatment. (h = hours; G = graphite bed powder; P = polished surface, R = resintered).

mechanism of this transformation is still unclear, future works are needed in order to study more in depth this theme considering that the extent of transformation of the *t*-ZrO₂ phase could be depending on factors such as nature of ceramic matrix (see Supplementary Fig. S2 for sample C3), amount and nature of the destabilizer as well as the sintering temperature (see Fig. S3 in Supplementary material) and time (see Fig. 2).

4. Conclusion

Herein, we have successfully demonstrated experimentally an unusual transformation of the *t*-ZrO₂ phase into *m*-ZrO₂ phase when ZTA composites with additions of few amount of multiwall carbon nanotubes are pressureless sintered in air using GP as bed powder. The possible transformation mechanism has been described. Moreover, this behavior could provide new insights into the performance of the zirconia based ceramics in the presence of CNTs. In this context, a more in depth study on this phenomenon in ZTA composites is in progress in order to provide more reliable information concerning to the transformation of the tetragonal zirconia into a monoclinic one.

Acknowledgments

The authors thank Professor Barry Muddle, National Key Centre for Advanced Materials Technology (CAMT), Monash University, Australia,

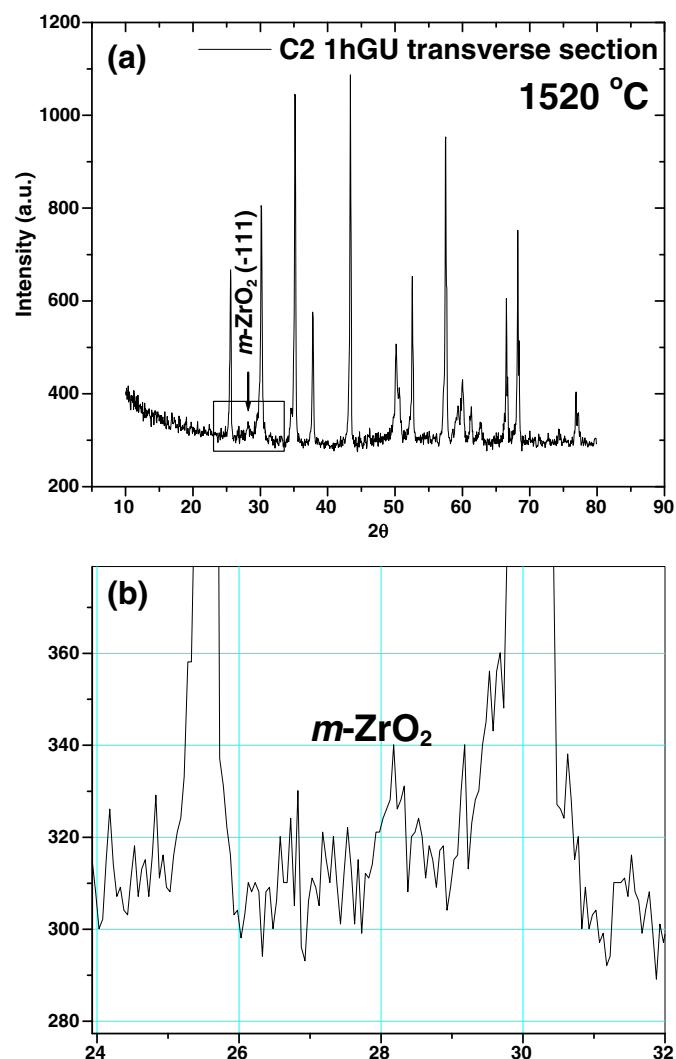


Fig. 5. XRD pattern corresponding to the transverse section of the sample C2 sintered at 1520 °C for 1 h (a). The peak corresponding to $(-111)_m$ plane is clearly observed in (b). (h = hours; G = graphite bed powder; U = unpolished surface).

for his help with the understanding of monoclinic phase formation in the samples.

Appendix A. Supplementary data

Supplementary data to this article can be found online at <http://dx.doi.org/10.1016/j.ijrmhm.2012.07.004>.

References

- [1] Cástorová K, Hadraba H, Cihlár J. Hydrothermal ageing of tetragonal zirconia ceramics. *Ceram Silik* 2004;48(3):85–92.
- [2] Chintapalli R, Mestra A, García Marro F, Yan H, Reece M, Anglada M. Stability of nanocrystalline spark plasma sintered 3Y-TZP. *Materials* 2010;3(2):800–14.
- [3] Mazaheri M, Mari D, Razabi Hesabi Z, Schaller R, Fantozzi G. Multi-walled carbon nanotube/nanostructured zirconia composites: outstanding mechanical properties in a wide range of temperature. *Compos Sci Technol* 2011;71(7):939–45.
- [4] Elshazly E, El-Hout SM, El-Sayed Ali M. Ytria tetragonal zirconia biomaterials: kinetic investigation. *J Mater Sci Technol* 2011;27(4):332–7.
- [5] Cheng Y, Thompson DP. Nitrogen-containing tetragonal zirconia. *J Am Ceram Soc* 1991;74(5):1135–8.
- [6] Luo TY, Liang TX, Li CS. Stabilization of cubic zirconia by carbon nanotubes. *Mater Sci Eng. A* 2004;366(1):206–9.
- [7] Bocanegra-Bernal MH, Echeberria J, Ollo J, Garcia-Reyes A, Domínguez-Rios C, Reyes-Rojas, et al. A comparison of the effects of multi-wall and single-wall carbon nanotube additions on the properties of zirconia toughened alumina composites. *Carbon* 2011;49(5):1599–607.
- [8] Kelly PM, Francis Rose LR. The martensitic transformation in ceramics – its role in transformation toughening. *Prog Mater Sci* 2002;47(5):463–557.
- [9] Luo TY, Liang TX, Li CS. Addition of carbon nanotubes during the preparation of zirconia nanoparticles: influence on structure and phase composition. *Powder Technol* 2004;139(2):118–22.
- [10] Wang DN, Liang KM. The effect of carbon on the phase stability of zirconia. *J Mater Sci Lett* 1998;17(4):343–4.